PHYSICAL REVIEW D VOLUME 27, NUMBER 6 15 MARCH 1983

Projector Monte Carlo method

R. Blankenbecler
Stanford Linear Accelerator Center, Stanford University, Stanford, California 94305

R. L. Sugar
Department of Physics and Institute for Theoretical Physics, University of California, Santa Barbara, California 93106

(Received 10 September 1982)

A simulation method for the calculation of properties of lattice field theories is studied. This method involves the numerical evaluation of projection operators onto low-lying quantum states. It is an alternative to the standard Monte Carlo evaluation of path integrals or the trace of the partition function and has many advantages. As an illustration, it is applied to a one-dimensional many-fermion system.

I. INTRODUCTION

The numerical simulation of lattice field theories has important applications to a wide variety of problems in high-energy and condensed-matter physics. In this paper we present an approach to this problem which involves the numerical evaluation of projection operators onto low-lying quantum states. This approach is an adaptation to lattice field theories of the Green's-function Monte Carlo method which has been applied with striking success to a variety of nonrelativistic many-body systems.[1] It was inspired by the recent work of Kuti on stochastic methods of matrix inversion and multiplication.[2,3]

We begin by briefly outlining our approach. In Sec. II, we will illustrate it by studying in detail a model of interacting fermions.

Let H be the Hamiltonian of interest. Then for sufficently large β, $e^{-\beta H}$ can be used as a projection operator onto the lowest energy state of a given symmetry or set of quantum numbers. For example, if E is the smallest eigenvalue of H whose eigenvector $|\psi\rangle$ is not orthogonal to the trial states $|\phi\rangle$ and $|\chi\rangle$, then

$$e^{-\Delta\beta E}=\lim_{\beta\to\infty}\frac{\langle\chi|e^{-(\beta+\Delta\beta)H}|\phi\rangle}{\langle\chi|e^{-\beta H}|\phi\rangle}\ . \tag{1}$$

Similarly, the expectation value of an operator Q in the state $|\psi\rangle$ is given by

$$\langle\psi|Q|\psi\rangle=\lim_{\beta\to\infty}\frac{\langle\chi|e^{-\beta H}Qe^{-\beta H}|\phi\rangle}{\langle\chi|e^{-2\beta H}|\phi\rangle}\ , \tag{2}$$

and the correlation function by

$$\langle\psi|Q(\tau)Q(0)|\psi\rangle=\lim_{\beta\to\infty}\frac{\langle\chi|e^{-\beta H}Qe^{-\tau H}Qe^{-\beta H}|\phi\rangle}{\langle\chi|e^{-(2\beta+\tau)H}|\phi\rangle}, \tag{3}$$

where

$$Q(\tau)=e^{\tau(H-E)}Qe^{-\tau(H-E)}\ . \tag{4}$$

Equations (1)—(3) form our starting point, and our objective is to numerically evaluate the various matrix elements appearing on their right-hand sides.

The first step is to break up β into L subintervals of width $\Delta\tau=\beta/L$. Then, following the recent work of Hirsch, Scalapino, and ourselves,[4] we write H as the sum of two Hamiltonians

$$H=H_1+H_2\ , \tag{5}$$

selected so that the matrix element of the operators

$$U(k)=e^{-\Delta\tau H_k}\quad(k=1,2) \tag{6}$$

are easy to evaluate. The choice of H_1 and H_2 of course depends on the particular system under consideration. We next note that

$$e^{-\Delta\tau H}=U(1)^{1/2}U(2)U(1)^{1/2}\{1-\tfrac{1}{6}(\Delta\tau)^3(\tfrac{1}{4}[H_1,[H_1,H_2]]-\tfrac{1}{2}[H_2,[H_2,H_1]])+\cdots\} \tag{7a}$$

$$=U(2)U(1)\{1-\tfrac{1}{2}(\Delta\tau)^2[H_2,H_1]+..\} . \tag{7b}$$

In most cases it is possible to replace the terms in curly brackets on the right-hand side of Eqs. (7a) and (7b) by the unit operator. That is the case for the models we study here. We shall make use of Eq. (7b) because it is somewhat easier to work with. It should be noted that $U(2)U(1)$ and $U(1)^{1/2}U(2)U(1)^{1/2}$ have the same eigenvalues, so there is no loss in accuracy in using Eq. (7b) rather than (7a) to compute energies. We do lose an order of $\Delta\tau$ in the computation of correlation functions and expectation values of operators, but this can be compensated for by working with sufficiently small values of $\Delta\tau$.

We now write

$$Y(\beta)=\langle\chi\,|\,e^{-\beta H}\,|\,\phi\rangle\cong\langle\chi\,|\,[U(2)U(1)]^L\,|\,\phi\rangle$$

$$=\sum_{i_{2L+1},i_{2L},\ldots,i_1}\langle\chi\,|\,i_{2L+1}\rangle\langle i_{2L+1}\,|\,U(2)\,|\,i_{2L}\rangle\langle i_{2L}\,|\,U(1)\,|\,i_{2L-1}\rangle\cdots\langle i_2\,|\,U(1)\,|\,i_1\rangle\langle i_1\,|\,\phi\rangle . \tag{8}$$

Similar expressions hold for the other matrix elements in Eqs. (1)—(3). In the last step of Eq. (8) we have introduced $2L+1$ complete sets of states which are to be chosen so as to simplify the matrix elements of $U(1)$ and $U(2)$. For example, for a single-particle Hamiltonian of the form $H=p^2+v(q)$, we might choose $H_1=p^2$, $H_2=v(q)$, and $|\,i_j\rangle$ to be the eigenstates of the momentum operator for j odd and the eigenstates of the coordinate operator for j even. Quite different breakups of H will be discussed in Sec. II.

We will perform the sum over intermediate states by applying the Monte Carlo method with importance sampling. We follow the recent work of Kuti[2,3] and write

$$\langle i\,|\,U(k)\,|\,j\rangle=S_{ij}(k)P_{ij}(k) , \tag{9}$$

where the $P_{ij}(k)$ are positive semidefinite and

$$\sum_i P_{ij}(k)=1 . \tag{10}$$

The exact form of the $P_{ij}(k)$ is at our disposal, and they can be chosen to optimize the rate of numerical convergence as will be discussed in Sec. II. The $P_{ij}(k)$ give the probability of making a transition from the state $|\,j\rangle$ to the state $|\,i\rangle$ through the operator $U(k)$. We shall refer to $S_{ij}(k)$ as the score for this particular transition.

Our procedure for evaluating matrix elements such as $Y(\beta)$ is as follows. We choose a specific state $|\,i_1\rangle$ with a probability proportional to $|\langle i_1\,|\,\phi\rangle|$. We then choose a specific $|\,i_2\rangle$ with a probability $P_{i_2 i_1}(1)$ and $|\,i_3\rangle$ with a probability $P_{i_3 i_2}(2)$, etc. Having generated a specific set of values for $i_1,i_2,\ldots,i_{2L+1}$, we assign it a weight

$$W(i_{2L+1},i_{2L},\ldots,i_2,i_1)$$

$$=\langle\chi\,|\,i_{2L+1}\rangle S_{i_{2L+1},i_{2L}}(2)\cdots S_{i_2,i_1}(1)s, \tag{11}$$

where $s=\pm1$ depending on the sign of $\langle i_1\,|\,\phi\rangle$. Clearly, if we carry out this procedure N times, then

$$Y(\beta)=\lim_{N\to\infty}\sum W(i_{2L+1},i_{2L},\ldots,i_2,i_1) , \tag{12}$$

where the sum is over the N different sets of values of $i_1,\ldots,i_{2L+1}$ that are generated. Formulas analogous to Eqs. (11) and (12) hold for all other matrix elements in Eqs. (1)—(3). Of course, in practical calculations, both N and β must be finite, but we have found rapid convergence in the models studied to date.

We believe that the approach we have just outlined has a number of advantages over standard Monte Carlo procedures. If the Hamiltonian describes a lattice field theory, then the intermediate state $|\,i_j\rangle$ could describe the field configuration at a particular (imaginary) time slice. In our procedure one need only store the state (field configuration) at that one time slice while in the standard Monte Carlo calculations one must simultaneously store it at all time slices. Thus, for a problem in three space and one time dimensions, one must store data from a three- rather than a four-dimensional lattice.

Even more important is the fact that each sweep through the lattice, i.e., each determination of the states $i_1,\ldots,i_{2L+1}$, yields a completely independent set of data. In the standard Monte Carlo method, one must sweep through the lattice a number of times to obtain independent field configurations on which to make measurements.

The present approach appears to be particularly useful for calculating vacuum expectation values and correlation functions, such as single-particle fermion Green's functions, which are difficult to study with standard Monte Carlo techniques. It cannot be used to study systems at finite temperature.

In Sec. II, we develop our formalism in detail for a system of interacting fermions in one space dimension. In Sec. III, we present numerical results for

the ground-state energy, gap, and correlation functions. In Sec. IV, we discuss our results and the extension of our method to other problems.

II. AN ILLUSTRATIVE EXAMPLE

To illustrate our approach we consider a one-dimensional model of interacting fermions with the Hamiltonian

$$H=\int dx\left[2t\psi^{\dagger}(x)\sigma_x\frac{1}{i}\frac{\partial}{\partial x}\psi(x)+\Delta\psi^{\dagger}(x)\sigma_z\psi(x)-2V[\psi^{\dagger}(x)\sigma_z\psi(x)]^2\right], \tag{13}$$

where σ_x and σ_z are the usual Pauli spin matrices, and $\psi(x)$ is a two-component spinor field operator. For $\Delta=0$, H is the Hamiltonian of the Gross-Neveu model with one flavor, while for $V=0$ it simply describes free, massive fermions.

For numerical calculations we must put the theory on a lattice. If we do so naively by writing (j denotes the lattice site)

$$H=\sum_j[-it\psi_j^{\dagger}\sigma_x(\psi_{j+1}-\psi_{j-1})+\Delta\psi_j^{\dagger}\sigma_z\psi_j-\tfrac{1}{2}V(\psi_j^{\dagger}\sigma_z\psi_j+\psi_{j+1}^{\dagger}\sigma_z\psi_{j+1})^2], \tag{14}$$

then we encounter the well-known spectrum-doubling problem. To avoid it we adopt the Kogut-Susskind procedure[5] of placing the upper components of ψ_j on even lattice sites and the lower components on odd ones by choosing

$$\psi_j=(-i)^j\begin{bmatrix}c_j\\0\end{bmatrix}\quad(j\text{ even}),\qquad \psi_j=(-i)^j\begin{bmatrix}0\\c_j\end{bmatrix}\quad(j\text{ odd}). \tag{15}$$

$c_j^{\dagger}$ and c_j satisfy the usual anticommutation relations and are, respectively, the creation and annihilation operators for a fermion on the jth lattice site. In terms of these operators the Hamiltonian takes the form

$$H=\sum_j[-t(c_j^{\dagger}c_{j+1}+c_{j+1}^{\dagger}c_j)+\Delta(-)^jc_j^{\dagger}c_j-\tfrac{1}{2}V(c_j^{\dagger}c_j-c_{j+1}^{\dagger}c_{j+1})^2]. \tag{16}$$

For $V=0$, this model can, of course, be solved analytically, so we have a check on our numerical results. For $\Delta=0$, the model is equivalent to the XXZ model whose properties are well understood. For $V>2t$, there is spontaneous breaking of chiral symmetry with a gap and order parameter that go exponentially to zero as $V\to 2t+$. For $0\le V<2t$ chiral symmetry is unbroken.

For our numerical calculation we work with a finite lattice with M spatial points. It is convenient to use periodic boundary conditions when an odd number of fermions are present, and antiperiodic ones when an even number are present. Of course, most quantities of interest are independent of the boundary conditions for sufficiently large M.

It is useful to write the Hamiltonian in the form

$$H=\sum_j h_{j,j+1} \tag{17}$$

with

$$h_{j,j+1}=-t(c_j^{\dagger}c_{j+1}+c_{j+1}^{\dagger}c_j)+\tfrac{1}{2}\Delta(-)^j(c_j^{\dagger}c_j-c_{j+1}^{\dagger}c_{j+1})-\tfrac{1}{2}V(c_j^{\dagger}c_j-c_{j+1}^{\dagger}c_{j+1})^2. \tag{18}$$

Following Ref. 4, we choose the breakup of Eq. (5) to be

$$H_1=\sum_{j\text{ odd}}h_{j,j+1},\qquad H_2=\sum_{j\text{ even}}h_{j,j+1}. \tag{19}$$

Thus, both H_1 and H_2 are given by a sum of commuting two-site operators, and $U(1)$ and $U(2)$ are each a product of two-site operators.

This type of breakup is useful for any problem with only nearest-neighbor interactions. If we choose the intermediate states in Eq. (8) to be ones in which the fermions are localized on specific lattice sites, then in generating the state $|i_{j+1}\rangle$ from $|i_j\rangle$ we need only consider one pair of lattice sites at a time, and we need only solve a two-site problem to calculate the matrix elements of $U(1)$ and $U(2)$. We denote by $|n_jn_{j+1}\rangle$ the state with n_j (n_{j+1}) fermions on site j ($j+1$). Then with

$$U_j=e^{-\Delta\tau h_{j,j+1}},$$

we find

$$\begin{aligned}U_j|0,0\rangle&=|0,0\rangle,\\ U_j|1,1\rangle&=|1,1\rangle,\\ U_j|1,0\rangle&=u_0^{+}|1,0\rangle+u_1|0,1\rangle,\\ U_j|0,1\rangle&=u_0^{-}|0,1\rangle+u_1|1,0\rangle,\end{aligned} \tag{20}$$

where

$$u_0^{\pm}=e^{1/2\Delta\tau V}[\mathrm{ch}\pm(-)^j(\Delta/2\epsilon)\mathrm{sh}]\ ,$$
$$u_1=e^{1/2\Delta\tau V}(t/\epsilon)\mathrm{sh}\ ,$$
$$\epsilon=(t^2+\Delta^2/4)^{1/2}\ , \tag{21}$$
$$\mathrm{ch}=\cosh(\Delta\tau\epsilon)\ ,$$
$$\mathrm{sh}=\sinh(\Delta\tau\epsilon)\ .$$

We are now in a position to perform the sums over intermediate states in Eq. (8). We work in the occupation number basis and denote by $|n_1n_2\cdots n_M\rangle$. The state in which there are n_1 fermions on site 1, n_2 on site 2, etc. Of course the n_i can only take on the values 0 and 1. We choose the initial configuration of the fermions with probability proportional to $|\langle n_1n_2\cdots n_M|\phi\rangle|$. For example, if we wish to obtain the ground state of the half-filled band, it is convenient to take

$$|\phi\rangle=\frac{1}{\sqrt{2}}[\,|1010\cdots\rangle+|0101\cdots\rangle\,] \tag{22}$$

since this is a translationally invariant state which is unlikely to be orthogonal to the ground state. We choose as our starting configuration each of the states on the right-hand side of Eq. (22) with equal probability. In order to calculate the fermion mass we need the lowest-energy, zero-momentum state with one more fermion than the half-filled band. We would then modify each term on the right-hand side of Eq. (22) by adding one extra fermion, locating it on each empty site with equal probability.

In applying the operator $U(1)$ to the initial configuration, we start with sites 1 and 2. If they are both empty or both filled, Eq. (20) indicates that no change is possible and the score is unity. If one of the sites is filled, the fermion may hop to the other one. We must choose the hopping probability, P, and its corresponding score so that their product is u_1. Similarly the product of the probability and score for the fermion to remain at its original site must be $u_0^{\pm}$ with the sign depending on whether the fermion is on site 1 or 2. We will discuss the choice of the hopping probability in a moment. Assuming that it has been fixed, we generate a random number, r, between zero and one, and have the fermion hop if $r<P$ and remain in its original position if $r>P$. We do not need to save the scores for each pair of sites, merely the total number of times each different score occurs. We next move on to sites 3 and 4, and repeat the procedure. After we have finished sites M-1 and M, we have the fermion configuration corresponding to the intermediate state $|i_2\rangle$ of Eq. (8).

We are now ready to apply the operator $U(2)$. The procedure is identical except the appropriate pairs of sites are (2,3), (4,5),.... In this way way we generate all the intermediate sites of Eq. (8); however, at any one time the computer need only store one fermion spatial configuration.

As long as we are interested in translationally invariant states, it is convenient to take the state $|\chi\rangle$ to be the sum over all occupation number states with equal weight. Then, no matter what the final configuration is, $\langle\chi|i_{2+1}\rangle$ will have the same value, which can be chosen to be unity.

It only remains to determine the hopping probability. It is important to keep in mind that only the product of the score and the probability is determined by the matrix elements of $U(k)$. The hopping probability itself can be chosen at our convenience so long as the scores are suitably adjusted. Let us focus on sites j and $j+1$, and assume that j is occupied and $j+1$ is not. From Eq. (20) we might be tempted to choose

$$P=(t/\epsilon)\mathrm{sh}\left[\mathrm{ch}+\mathrm{sh}\left[t+\frac{\Delta}{2\epsilon}(-)^j\right]\right]^{-1}\ . \tag{23}$$

However, we would then be ignoring possibly important repulsive effects due to the Pauli principle and the interaction, which would arise if there were fermions on sites $j-1$ and $j+2$. To estimate how such effects would influence the matrix elements of interest, we multiply $U(k)$ on the left by the operator

$$\theta_T=\exp\{\tfrac{1}{2}\Delta\tau V_T[\,(c_j^{\dagger}c_j-n_{j-1})^2 + (c_{j+1}^{\dagger}c_{j+1}-n_{j+2})^2-1]\}\ . \tag{24}$$

Here n_{j-1} and n_{j+2} are the occupation numbers for sites $j-1$ and $j+2$ (1 if they are occupied and 0 if they are not), and V_T is a trial parameter that is at our disposal. The operator θ_T helps to "smooth out" the breakup of H into H_1 and H_2. The last two lines of Eq. (20) now become

$$\theta_T U_i|1,0\rangle=gu_0^{+}|1,0\rangle+g^{-1}u_1|0,1\rangle\ ,$$
$$\theta_T U_i|0,1\rangle=g^{-1}u_0^{-}|0,1\rangle+gu_1|1,0\rangle\ , \tag{25}$$

where

$$g=\exp[-\tfrac{1}{2}\Delta\tau V_T(n_{j-1}-n_{j+2})]\ . \tag{26}$$

We use Eq. (25) to determine the probabilities. If site j is initially occupied, we take the hopping probability to be

$$P=g^{-1}u_1/(gu_0^{+}+g^{-1}u_1) \tag{27}$$

and the corresponding score is $g^2u_0^{+}+u_1$. If site $j+1$ is initially occupied, we use Eq. (27) with the substitutions $g\to g^{-1}$ and $(-)^j\to(-)^{j+1}$. The trial

parameter V_T is adjusted to optimize the rate of numerical convergence. One can, of course, make more elaborate parametrizations of the hopping probability, but the present one is quite sufficient for this problem. Note that P depends on V_T but not on V.

When the infinite system has a degenerate ground state, which is the case for when $\Delta=0$ and $V>2t$, then one of the interesting quantities to calculate is the vacuum expectation value (VEV) of the order parameter. In our model the order parameter is

$$Q=M^{-1/2}\sum_j \psi_j^\dagger \sigma_x \psi_j = M^{-1/2}\sum_j (-)^j c_j^\dagger c_j \ . \tag{28}$$

The symmetry that is spontaneously broken when Q obtains a vacuum expectation value is chiral invariance, which in the Kogut-Susskind formalism corresponds to translation by a single lattice site. Let O be the operator corresponding to this translation. Then

$$\begin{aligned} OHO^{-1}&=H \ , \\ OQO^{-1}&=-Q \ . \end{aligned} \tag{29}$$

Of course, there can be no spontaneous symmetry breaking on a finite lattice which is why it is difficult to make a good measurement of the VEV of the order parameter by standard Monte Carlo methods. For large lattices the two lowest energy states will be nearly degenerate. We expect them to have opposite parity under O so we denote them by $|\psi_\pm\rangle$ with

$$O|\psi_\pm\rangle=\pm|\psi_\pm\rangle \ . \tag{30}$$

Now $\langle\psi_-|Q|\psi_+\rangle$ will be finite on a finite lattice, and it will approach the VEV of the order parameter as the lattice becomes large. To calculate this quantity it is convenient to make use of two initial trial states

$$|\phi_\pm\rangle=\frac{1}{\sqrt{2}}[\,|1010\cdots\rangle\pm|0101..\rangle\,] \tag{31}$$

so that $O|\phi_\pm\rangle=\pm|\phi_\pm\rangle$. It is then easy to see that

$$|\langle\psi_-|Q|\psi_+\rangle|^2=\lim_{\beta\to\infty}\frac{N(\beta)}{D(\beta)} \ , \tag{32}$$

where

$$\begin{aligned} N(\beta)=&\langle\chi|Qe^{-\beta H}Qe^{-\beta H}|\phi_+\rangle \\ &\times\langle\chi|e^{-\beta H}Qe^{-\beta H}|\phi_-\rangle \end{aligned} \tag{33}$$

and

$$D(\beta)=\langle\chi|e^{-2\beta H}|\phi_+\rangle\langle\chi|Qe^{-2\beta H}|\phi_-\rangle \ . \tag{34}$$

Vacuum expectation values of other quantities that are odd under O can be obtained by similar manipulations. Note that all these quantities can be measured with the same set of runs by keeping separate scores. The same set of matrix elements give us a direct measurement of E_+-E_-, thereby allowing us to make an approximate determination of where degeneracy occurs.

III. NUMERICAL RESULTS

In this section, we shall apply our proposed method to the model worked out in the previous section. The results will be compared to the exact values where known, and to previous calculations using the canonical distribution approach, where appropriate. Most of the numerical results are from computer runs with 4000 data passes to collect the scores for the numerators and denominators. This was then repeated and the data averaged.

The first comparison will be to energies and gaps. For most of the following calculation we have chosen $\Delta\tau=\frac{1}{4}$ and will give some results for other $\Delta\tau$ values. In Table I, the results for $V=0$ and $\Delta=0,0.5,1.0$ for two lattices are given. Since this is a free massive fermion problem, the exact results are known and are also given. The energies are energies per site, while the gap is the total energy difference between the half-filled band and the state with one extra fermion of mass Δ.

To explore the $\Delta\tau$ and β $(=L\Delta\tau)$ dependence of the numerical results for the ground-state energy density, values of $E_0(2L,\Delta\tau,\beta)$ for different choices of $\Delta\tau$ and $2L$ were computed for $\Delta=0, V=0$. Consider first the β dependence at fixed $\Delta\tau$,

$$\begin{aligned} &E_0(4,\tfrac{1}{4},\tfrac{1}{2})=-0.668\,8(3) \ , \\ &E_0(8,\tfrac{1}{4},1)=-0.651\,7(3) \ , \\ &E_0(16,\tfrac{1}{4},2)=-0.644\,2(5) \ , \\ &E_0(32,\tfrac{1}{4},4)=-0.642(1) \end{aligned} \tag{35}$$

and

$$\begin{aligned} &E_0(8,\tfrac{1}{8},\tfrac{1}{2})=-0.673\,3(6) \ , \\ &E_0(16,\tfrac{1}{8},1)=-0.652\,5(5) \ , \\ &E_0(24,\tfrac{1}{8},\tfrac{3}{2})=-0.646\,2(3) \ , \\ &E_0(32,\tfrac{1}{8},2)=-0.643\,9(5) \ , \end{aligned} \tag{36}$$

whereas $E_0(\text{exact})=-0.640\,7$. The numbers in parentheses are the statistical fluctuations in the last figure given. The $\Delta\tau$ dependence at fixed β is illustrated by the set

TABLE I. Energy density and gaps. The ground-state energy density of the half-filled band, E_0, and of the half-filled band plus one extra fermion, E_1, for the Hamiltonian of Eq. (16) with $V=0$. The gap is the difference in total energy of these states as measured on the finite lattice. The numbers in parentheses next to the Monte Carlo results are the statistical fluctuations in the last figure given.

	MC results			Exact results		
Δ	$-E_0$	$-E_1$	Gap	$-E_0$	$-E_1$	Gap
			$M=8,\ 2L=16$			
0	0.655(1)	0.606(1)	0.40(1)	0.653	0.604	0.40
0.5	0.712(2)	0.633(2)	0.63(2)	0.707	0.633	0.59
1.0	0.840(3)	0.713(3)	1.02(3)	0.840	0.713	1.02
			$M=16,\ 2L=16$			
0	0.644(1)	0.629(1)	0.24(2)	0.641	0.628	0.20
0.5	0.706(2)	0.674(2)	0.51(4)	0.702	0.670	0.51
1.0	0.841(3)	0.775(2)	1.06(6)	0.839	0.776	1.00

$$E_0(4,\tfrac{1}{2},1)=-0.6549(8)\ ,$$
$$E_0(8,\tfrac{1}{4},1)=-0.6517(3)\ , \qquad (37)$$
$$E_0(16,\tfrac{1}{8},1)=-0.6525(5)\ .$$

We have also computed the ground-state energies for the XXZ model with $\Delta=0$ and $V=1,2$. The results for $M=16$, $2L=16$, and $\Delta\tau=\frac{1}{4}$ are

$$E(V=1)=-1.404(1)\ ,$$
$$E(V=2)=-2.254(3)\ . \qquad (38)$$

The numerical results using the method of Ref. 4 for the above values of the coupling V are $-1.410(2)$ and $-2.240(4)$, respectively. These were computed from the canonical distribution and hence are the average thermal energies rather than the ground-state values.

We turn now to a measurement of the correlation function of the "staggered" order parameter, Q, of Eq. (28). We are interested in

$$\langle Q(\tau)Q(0)\rangle=\langle Q(J\Delta\tau)Q(0)\rangle\equiv C(J)\ . \qquad (39)$$

This function can be computed for the free field case of $V=0$, any Δ. The result of this comparison is given in Table II for $M=16$, $2L=32$, and $\Delta=0$. The correlation function does not rise past the midpoint of L as it does when using the (periodic) partition-function method.

As a final example, we turn to the evaluation of the single-particle Green's function and its Fourier transform. This is a function that is difficult to evaluate using the standard partition-function approach but is quite straightforward using the projection method.[6] Defining the equal-time spatial

TABLE II. Correlation function. The correlation function $C(J)$ defined in Eq. (39) for the Hamiltonian of Eq. (16) with $\Delta=V=0$. The subscripts EX and MC refer to exact and Monte Carlo results, respectively. The numbers in parentheses next to the Monte Carlo results are the statistical fluctuations in the last figures given.

J	$C(J)_{\mathrm{MC}}$	$C_{\mathrm{EX}}(J)$
0	0.507(10)	0.500
1	0.276(12)	0.276
2	0.168(38)	0.167
3	0.113(31)	0.110
4	0.095(25)	0.078
5	0.055(25)	0.058
6	0.039(44)	0.044
7	0.030(30)	0.035

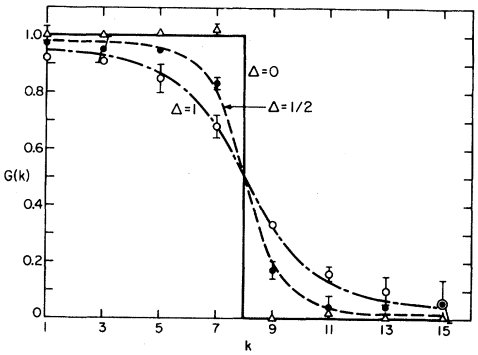

FIG. 1. The Fourier transform of the single-particle Green's function, $\tilde{G}(k)$, defined in Eq. (41) for the Hamiltonian of Eq. (16) with $V=0$ and $\Delta=0,\frac{1}{2},1$. The curves are exact results. The triangles are the Monte Carlo result for $\Delta=0$, the solid circles for $\Delta=\frac{1}{2}$, and the hollow circles for $\Delta=1$. When no error bars are given, the statistical errors are smaller than the symbols.

TABLE III. Green's function. The single-particle Green's function $G(J)$ and its Fourier transform $\tilde{G}(k)$ defined in Eqs. (40) and (41) with $\Delta=0$. The subscripts EX and MC refer to exact and Monte Carlo results, respectively. The numbers in parentheses next to the Monte Carlo results are the statistical fluctuations in the last figure given.

J	G_{EX} $(V=0,J)$	G_{MC} $(V=0,J)$	G_{MC} $(V=1,J)$	G_{MC} $(V=2,J)$
1	0.320	0.322(5)	0.293(10)	0.24(5)
2	0	0.000(4)	0.006(13)	0.01(1)
3	−0.112	−0.120(5)	−0.090(3)	−0.05(1)
4	0	0.003(5)	0.003(4)	0.004(2)
5	0.075	0.078(5)	0.063(2)	0.017(2)
6	0	0.000(3)	0.001(4)	−0.003(3)
7	−0.064	−0.065(5)	−0.047(1)	−0.014(3)
8	0	0.000(3)	0.001(5)	−0.001(2)

k	$\tilde{G}_{EX}$ $(V=0,k)$	$\tilde{G}_{MC}$ $(V=0,k)$	$\tilde{G}_{MC}$ $(V=1,k)$	$\tilde{G}_{MC}$ $V(=2,k)$
1	1	0.998(28)	0.97(5)	0.93(9)
3	1	0.998(7)	0.94(3)	0.91(8)
5	1	1.010(7)	0.95(1)	0.84(7)
7	1	1.022(15)	0.93(3)	0.70(2)
9	0	−0.012(8)	0.11(3)	0.28(2)
11	0	−0.019(20)	0.05(2)	0.13(6)
13	0	−0.007(12)	0.04(1)	0.10(9)
15	0	0.010(10	0.02(1)	0.11(11)

Green's function as

$$G(J)=M^{-1}\sum_i \langle c^\dagger_{i+J} c_i \rangle \tag{40}$$

and its Fourier transform

$$\tilde{G}(k)=\tilde{G}(-k)=\langle c^\dagger_k c_k \rangle \ , \tag{41}$$

the calculation proceeds as outlined in Sec. II. The Green's function will be evaluated for $M=16$, $2L=16$ and for various Δ and V values.

With the definition of Eq. (41) the exact $G(J)$ vanishes for J even. This provides one test of our numerical results. Let us first examine the test case $V=0$ at various Δ. The numerical results for the case $V=0=\Delta$ are given in Table III, and are in good agreement with the exact values.

Now consider the results for the Green's function for $\Delta=0$ and $V=1,2$ given in the right-hand columns of Table III. As V increases, $\tilde{G}(k)$ becomes rounded at the Fermi surface. When $V=2$, the critical value at which a mass gap starts to develop, $\tilde{G}(k)$ begins to look more like the Green's function for a finite fermion mass Δ. The numerical results for $\tilde{G}(k)$ for the values $\Delta=0$, $\frac{1}{2}$ and 1 are given in Fig. 1 and compared to the exact values.

Finally, we have computed the matrix element of the operator Q between the ground state and the lowest state that it connects to. For $V>2$, these states become degenerate and $\langle \psi_- | Q | \psi_+ \rangle$ is the order parameter. The numerical results for $M=16$, $2L=16$ are

V	$\lvert\langle \psi_- \lvert Q \rvert \psi_+ \rangle\rvert^2$
1	0.06(2)
1.5	0.10(1)
2	0.15(1)
2.5	0.18(1)

(42)

which are in good agreement with the results of Ref. 4.

IV. CONCLUSION

The projector method presented here appears to be a fast, stable, and efficient way to compute the properties of the lowest states of a quantum system. It is particularly convenient for computing energy gaps and fermion Green's functions which are sometimes difficult to extract in conventional Monte Car-

lo calculations.

The method has a number of advantages. (i) It is simple to implement. Each Monte Carlo step requires a minimal number of lookups and algebraic operations. (ii) It requires less storage space then conventional Monte Carlo evaluations of path integrals because it is only necessary to store the state, or field configuration at a single (imaginary) time slice. (iii) Each sweep through the lattice (i.e., through the $2L$-time steps) is statistically independent, and yields useful data. It is not necessary to make a number of passes through the lattice to obtain independent configurations as in standard Monte Carlo calculations. (iv) The trial parameters in the operator θ_T can be chosen to improve the rate of convergence. One can introduce knowledge of the physics into the transitions probabilities while keeping the calculation exact by using correct values for the scores. The initial state $|\phi\rangle$ can be used as variational trial function and adjusted to speed the convergence.

As we previously noted, the hopping probability is independent of the coupling constant in the model studied in this paper, and it can always be chosen so in more general models. The dependence on the coupling constant comes in only through the scores. This means that one can directly evaluate derivatives of the energy and of matrix elements with respect to the coupling constant (or other parameter appearing in the Hamiltonian) without the loss of accuracy associated with numerical differentiation. Another advantage of the independence of the hopping parameter of the coupling constant is that one can evaluate energies and matrix elements for a range of couplings from a single set of configurations. Of course, it may not be possible to obtain satisfactory statistics for the entire range of couplings of interest from a single set of trial parameters, but in the present model, one value of the trial parameters did suffice for a considerable range of couplings. The important point is that one spends far more computer time generating configurations than computing scores, so it always pays to compute several observables for a particular configuration.

One can also use the Feynman-Hellmann theorem to compute derivatives of the energy with respect to parameters occurring in the Hamiltonian, i.e.,

$$dE(g)/dg = \langle \psi(g) \,|\, \partial H/\partial g \,|\, \psi(g) \rangle \ ,$$

where the expectation value is computed directly.

Presently, we have programs running for two quantum spin models in two space dimensions. These are the anisotropic Heisenberg (spin-$\frac{1}{2}$) model and the Ising model in a transverse field. For these cases, the data rate is extremely fast compared to standard Monte Carlo techniques. The energy in the Ising model has been studied recently using the stochastic method by Kuti and Polonyi.[3] A full discussion of our results for these problems will appear elsewhere.[7]

ACKNOWLEDGMENTS

We would like to express our appreciation to J. Kuti who inspired this work. We would also like to thank E. Dahl, J. Hirsch, and D. Scalapino for helpful conversations, and P. Kunz and SLAC Group B for their assistance and access to the 168/E processor where most of the numerical work was done. This work was supported in part by National Science Foundation Grants Nos. PHY77-27084 and PHY80-18938 and by the U. S. Department of Energy under Contract No. DE-AC03-763-F00515.

[1]M. Metropolis and S. Ulam, J. Am. Stat. Assoc. 44, 335 (1949); J. B. Anderson, J. Chem. Phys. 63, 1499 (1975); 65, 4121 (1976); 73, 3897 (1980); 74, 6307 (1981); D. M. Cepereley and B. J. Alder, Phys. Rev. Lett. 45, 560 (1980); P. J. Reynolds, D. M. Cepereley, B. J. Adler, and W. A. Lester, J. Chem. Phys. (to be published); J. W. Moskowitz, K. E. Schmidt, M. A. Lee, and M. H. Kalos, J. Chem. Phys. 77, 349 (1982); M. H. Kalos, D. Levesque, and L. Verlet, Phys. Rev. A 9, 2178 (1974); D. M. Cepereley and M. H. Kalos, in *Monte Carlo Methods in Statistical Physics,* edited by K. Binder (Springer, Berlin, 1979).

[2]J. Kuti, Phys. Rev. Lett. 49, 183 (1982).

[3]J. Kuti and J. Polonyi, paper submitted to the XXIth International Conference on High Energy Physics, Paris, 1982 (unpublished).

[4]J. Hirsch, D. Scalapino, R. Sugar, and R. Blankenbecler, Phys. Rev. Lett. 47, 1628 (1981); Phys. Rev. B 26, 5033 (1982).

[5]J. Kogut and L. Susskind, Phys. Rev. D 11, 395 (1975).

[6]Such Green's function have been calculated using the Green's-function Monte Carlo method by P. A. Whitlock, M. H. Kalos, G. V. Chester, and D. M. Cepereley [Phys. Rev. B 19, 5598 (1979)].

[7]R. Blankenbecler, E. D. Dahl. J. Hirsch, D. Scalapino, and R. Sugar (in preparation).